Neutrosophic Knowledge, Vol. 10, 2026
University of New Mexico

Article

Finitesimally Punctured Waves, Surfaces, and Manifolds: Connections and Applications

Florentin Smarandache [1] *

[1] Emeritus Professor, Department of Mathematics & Sciences University of New Mexico, Gallup, NM 87301, USA, , https://fs.unm.edu/IPW/, e-mail: smarand@unm.edu

* Correspondence: e-mail: smarand@unm.edu

Received: 03, 19, 2026; *Accepted:* 03, 25, 2026

Abstract

The Finitesimally Punctured Wave (FPW) — introduced in Smarandache (2026) as the practical, experimentally accessible counterpart of the Infinitesimally Punctured Wave (IPW) — replaces the formal mathematical infinitesimal separation ε between sub-particles with a genuine positive real distance $\delta > 0$. This paper develops the full landscape of connections between the FPW program and established theories across physics, mathematics, and technology, and charts a broad application horizon for the companion structures: Finitesimally Punctured Surfaces (FPS) and Finitesimally Punctured Manifolds (FPM). We show that every crystal lattice, photonic crystal, phononic crystal, and quantum dot array is already a FPW; that graphene and 2D materials are FPS; that lattice QCD and causal set theory are FPM; and that loop quantum gravity, non-commutative geometry, holographic AdS/CFT, and topological quantum computing all have natural FPW/FPS/FPM realizations. On the application side we identify new research directions in metamaterial engineering, quantum error correction, post-quantum cryptography, neural-network theory, cosmological structure formation, and biological physics. Throughout, the Neutrosophic T-I-F decomposition of the FPW provides the logical bridge between continuous and discrete descriptions.

Keywords: Finitesimally Punctured Wave; FPW; FPS; FPM; lattice physics; condensed matter; topological insulators; metamaterials; quantum computing; neutrosophic logic; quantum gravity; AdS/CFT; neural networks; cryptography; causal set theory; loop quantum gravity; non-commutative geometry.

1. Introduction

The Infinitesimally Punctured Wave (IPW) program, initiated by Smarandache in 2019, proposes that every quantum entity is an aggregation of infinitely many sub-particles arranged along a wave-shaped path, with consecutive sub-particles separated by an infinitesimal gap $\varepsilon \to 0$ in the sense of nonstandard analysis. The resulting theory resolves wave–particle duality, eliminates wavefunction collapse, provides a natural UV regulator via the Puncture Buffering Principle, and offers singular-free black holes and a non-singular cosmological bounce.

The Finitesimally Punctured Wave (FPW) extends this framework from the virtual mathematical world (infinitesimal ε) to the real physical world (genuine positive real $\delta > 0$). The transition $\varepsilon \to \delta$ is the transition from a perfect theoretical ideal to an experimentally accessible theory with measurable predictions: a hard Brillouin-zone UV cut-off at $k_{max} = \pi/\delta$, a minimum position uncertainty $\Delta x_{min} \approx \delta/\pi$, and a modified dispersion relation that deviates from the linear standard-QM relation at wave vectors $k \sim 1/\delta$.

This paper asks: what are the connections of the FPW to established theories, and what new applications become possible? We organize our answer into three main parts: (I) connections to established physics and mathematics; (II) FPS (Finitesimally Punctured Surfaces) and FPM (Finitesimally Punctured Manifolds) — the 2D and n-dimensional generalizations; and (III) new application fields enabled by the FPW/FPS/FPM language.

Throughout, we use the Neutrosophic T-I-F decomposition of every FPW/FPS/FPM structure: T encodes the smooth, wave-like, classical regime; F encodes the localized, particle-like, singular regime at each puncture; and I encodes the transition zone of finite thickness δ — which, unlike the infinitesimal IPW transition, is a real physical length accessible to experiment.

2. The Finitesimally Punctured Wave: Core Definitions and Equations

2.1 Fundamental Definition

Definition: Finitesimally Punctured Wave (FPW)

A quantum entity or physical wave modeled as an ordered set

$$S_\delta = \{ p_1, p_2, \ldots, p_N \}$$

of N sub-particles arranged along a wave-shaped path, with each consecutive pair (p_k, p_{k+1}) separated by the fixed real distance $\delta > 0$.

Total sub-particle count: $N = L / \delta$ for a wave of path-length L.

The wave function is the density envelope sampled at sites $\{ k \cdot \delta : k = 1,\ldots,N \}$.

Regime: the FPW looks like a continuous wave for probe resolution R >> δ,
and reveals discrete lattice structure at R ~ δ.

The key distinction from the IPW is that δ is an ordinary real number — small, perhaps sub-Planckian, but measurable in principle. The IPW's ε is a hyperreal with standard part zero; the FPW's δ belongs to the standard real line $\mathbb{R}$.

2.2 The FPW Discrete Field Equation

The evolution of the FPW sub-particle amplitudes φ_k(t) is governed by the Discrete Nonlinear Schrödinger Equation (DNLSE):

Eq. (2.1) — FPW Discrete Field Equation (DNLSE)

$$i\hbar \cdot d\varphi\_k/dt \;=\; -J \cdot (\varphi\_\{k+1\} + \varphi\_\{k-1\} - 2\varphi\_k) / \delta^2 \;+\; U\_k \cdot \varphi\_k \;+\; g|\varphi\_k|^2 \cdot \varphi\_k$$

$$where{:}\; J \;=\; nearest-neighbor\ coupling\ constant\ (wave\ "tension")$$

$$U\_k \;=\; external\ potential\ at\ site\ k$$

$$g|\varphi\_k|^2 \;=\; self-interaction\ (FPW\ puncture\ regulariser)$$

$$Continuum\ limit{:}\; \delta \to 0\ with\ J \;=\; \hbar^2/(2m\delta^2)\ \ held\ fixed$$

→ reduces to the standard nonlinear Schrödinger equation

2.3 FPW Dispersion Relation

For a free FPW (no external potential, linear regime), plane-wave solutions φ_k = exp(i(kδ·q − ωt)) give:

Eq. (2.2) — FPW Dispersion Relation

$$\omega(q) \;=\; (2J/\hbar) \cdot [1 - cos(q\delta)] / \delta^2$$

$$Long-wavelength\ limit\ (q\delta << 1){:}$$

$$\omega \;\approx\; J \cdot q^2/\hbar \cdot [1 - (q\delta)^2/12 + \ldots] \quad (standard\ QM\ recovered)$$

$Short-wavelength\ saturation\ (q\delta \sim 1)$:
$\omega\_max \ = \ 4J\ /\ (\hbar\delta^2)$ $\quad (natural\ UV\ cut-off)$
$Brillouin\ zone\ boundary$: $q\_max \ = \ \pi/\delta$
$Minimum\ wavelength$: $\quad \lambda\_min \ = \ 2\delta \quad (Nyquist\ limit\ of\ FPW\ lattice)$

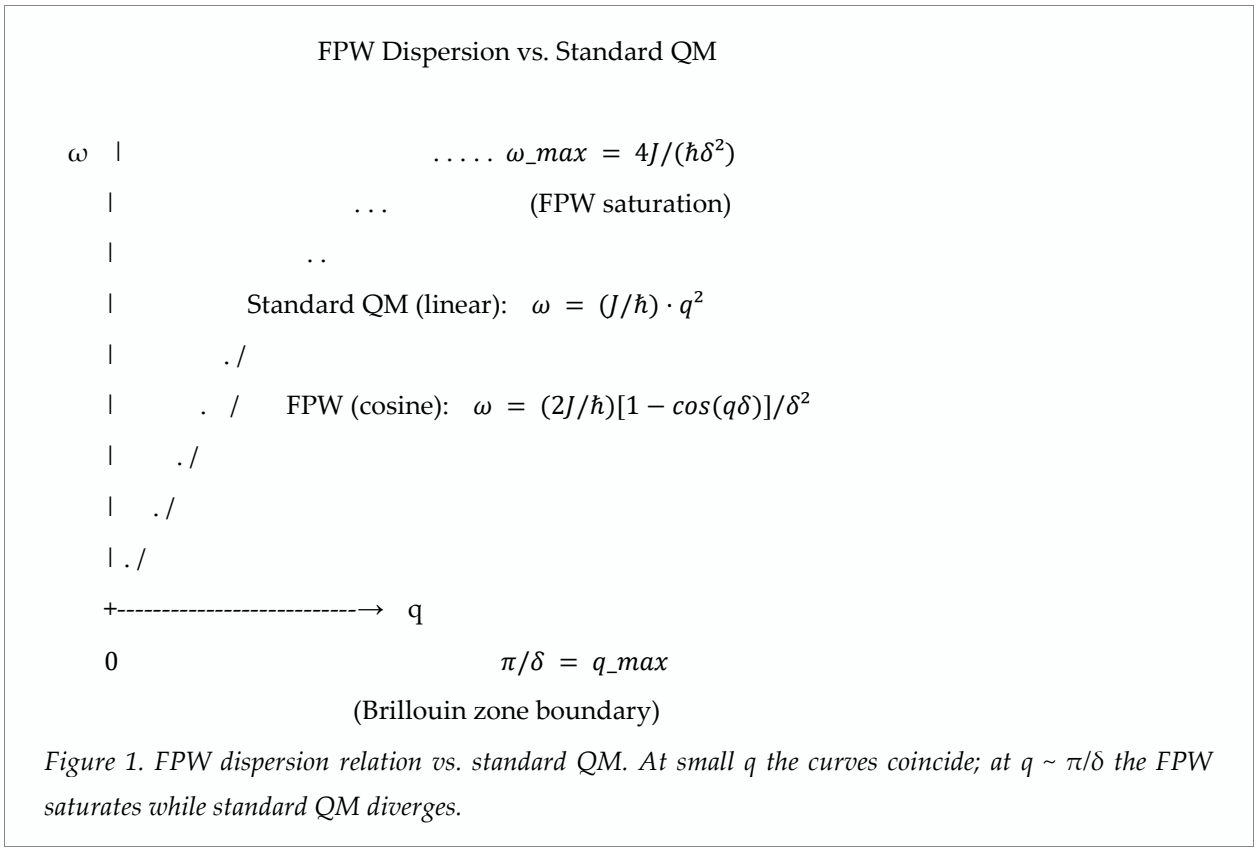

Figure 1. FPW dispersion relation vs. standard QM. At small q the curves coincide; at q ~ π/δ the FPW saturates while standard QM diverges.

2.4 Modified Uncertainty Relations

The FPW lattice modifies the Heisenberg uncertainty principle. Because position is discrete (values at lattice sites kδ) and momentum has a hard cut-off at $p_{max} = \pi\hbar/\delta$, the generalized uncertainty relation becomes:

Eq. (2.3) — FPW Generalized Uncertainty Principle (GUP)
$\Delta x \cdot \Delta p \ \geq \ (\hbar/2) \cdot [1 + (\Delta p / p_{max})^2]$

$$= (\hbar/2) \cdot [1 + (\Delta p \cdot \delta / (\pi\hbar))^2]$$

Minimum position uncertainty (at $\Delta p \to p_{max}$):

$$\Delta x_{min} \approx \delta/\pi \qquad \text{(hard minimum length = one lattice cell)}$$

This GUP with quadratic correction in Δp is a real, measurable prediction of the FPW — one that standard QM does not contain, and that reduces to the standard HUP in the limit $\delta \to 0$.

3. Connections to Established Physics and Mathematics

3.1 Condensed Matter: Lattice Physics and Topological Insulators

The most immediate realization of the FPW is in condensed matter physics. Every crystal lattice — with atoms separated by lattice constant a — is a FPW with $\delta = a$. The Debye model of phonons is a FPW with the Debye cut-off $q_D = \pi/a$ being exactly the FPW Brillouin zone boundary $q_{max} = \pi/\delta$. The FPW framework inverts the usual logic of condensed matter theory: instead of saying "a crystal approximates a continuum", it says "a continuum is the $\delta \to 0$ limit of a physically real FPW."

The connection to topological insulators is particularly deep. Topological insulators are materials where the bulk band structure carries a non-trivial topological invariant (Chern number or Z_2 index), leading to protected conducting surface states. In FPW language, these topological invariants are the F-component of the Neutrosophic Euler characteristic χ_N of the FPW lattice:

Eq. (3.1) — Neutrosophic Euler Characteristic of a FPW Lattice

$$\chi_N(\text{FPW lattice}) = (T, I, F)$$

T-component: classical smooth-regime contribution (bulk band topology)

I-component: transition-zone contributions (near Brillouin zone boundary)

F-component: defect/puncture contributions (topological invariant = Chern number)

Topological phase transition = discontinuous jump in F-component of χ_N

3.2 Quantum Field Theory and Lattice Gauge Theory

Lattice QCD (quantum chromodynamics on a discrete spacetime lattice with spacing a ~ 0.1 fm) is literally a four-dimensional FPW. Quark and gluon fields are defined at FPW lattice sites; the continuum limit is recovered as a → 0 (the FPM continuum limit). The FPW framework provides a physical ontological interpretation for what lattice QCD is doing: computing in the real FPW world (finite δ) and extrapolating toward the virtual IPW world (δ → 0).

The FPW dispersion relation also clarifies the famous Nielsen-Ninomiya fermion doubling problem in lattice QFT: naive lattice fermions produce 2^d spurious copies at the Brillouin zone corners (q = π/δ in each dimension). The Wilson, domain-wall, and overlap fermion actions are different ways of handling the FPW I-component at the zone boundary — they correspond to different choices of the indeterminacy treatment at k_max = π/δ.

3.3 Non-Commutative Geometry (Connes)

Alain Connes' non-commutative geometry replaces the continuous manifold of spacetime with a spectral triple (A, H, D) — an algebra A, Hilbert space H, and Dirac operator D — from which geometry is reconstructed algebraically. The FPW provides a commutative but discrete analog: the algebra is C(M_δ) (continuous functions on the FPW lattice manifold M_δ), and the Dirac operator is the discrete lattice Dirac operator D_δ. The FPW distance function is:

Eq. (3.2) — FPW Distance Function and Connection to Connes Spectral Triple
$d_\delta(x, y)$ = minimum path length through the FPW lattice connecting x and y
(measured in units of δ)
As $\delta \to 0$: $d_\delta \to d_{continuous}$ and $D_\delta \to D_{Dirac}$
The FPW is thus a discretization of Connes' spectral triple that is both
mathematically rigorous and physically motivated by the sub-particle structure.

3.4 Causal Set Theory (Sorkin, Bombelli)

Causal set theory proposes that spacetime is fundamentally a discrete partially-ordered set of spacetime events, with the continuous Lorentzian manifold emerging as an approximation. The

Planck-scale FPW with $\delta = l_P$ is precisely a causal set: each sub-particle is a spacetime event, and the FPW ordering (sub-particle k precedes sub-particle k+1) provides the causal structure. The FPW adds three new elements to causal set theory:

- A specific wave equation (the DNLSE, Eq. 2.1) governing the dynamics of the causal set.
- A physical interpretation of causal set elements as FPW sub-particles.
- A Neutrosophic T-I-F logical structure for the transition between causal and non-causal regions.

3.5 Loop Quantum Gravity (LQG)

In LQG, the geometry of space is quantized into spin networks whose edges carry quantum numbers j representing quantized areas. The minimum non-zero area eigenvalue is:

Eq. (3.3) — FPW Spacing from LQG Minimum Area
$A_{min} = 8\pi \cdot \gamma \cdot l_P^2 \cdot \sqrt{(j_{min}(j_{min} + 1))}$
where γ is the Barbero-Immirzi parameter and $l_P \approx 1.6 \times 10^{-35}$ m.
FPW connection: setting $\delta^2 = A_{min}$ gives $\delta = \sqrt{\gamma} \cdot l_P$
FPW dispersion corrections:
$\Delta\omega/\omega \approx -(k\delta)^2/12 = -(k \cdot \sqrt{\gamma} \cdot l_P)^2 / 12$
This matches the Planck-scale dispersion corrections predicted by LQG for photon propagation.

3.6 Holography and AdS/CFT Correspondence

The AdS/CFT correspondence (Maldacena) equates a (d+1)-dimensional gravitational theory in Anti-de Sitter space with a d-dimensional conformal field theory on its boundary. A FPW lattice regulator on the bulk AdS space with spacing δ_{bulk} induces a UV cut-off on the boundary CFT at $k_{max} = \pi/\delta_{boundary}$. The holographic renormalization group — integrating out bulk degrees of freedom from the AdS boundary inward — becomes the FPW continuum limit (taking $\delta \to 0$ from the

boundary into the bulk). The FPW provides a natural geometric implementation of holographic renormalization without additional regularization schemes.

3.7 Wavelet Theory and Multi-Resolution Analysis

Wavelet analysis (Daubechies, Mallat) decomposes a signal into components at different resolution scales. The FPW is a physical multi-resolution structure: at resolution $R \gg \delta$ it looks like a continuous wave; at $R \sim \delta$ the discrete lattice is visible. The FPW sub-particle amplitudes $\{\varphi_k\}$ are the wavelet coefficients of the physical wave at scale δ:

Eq. (3.4) — FPW as Physical Wavelet Decomposition
FPW as wavelet decomposition:
$\{\varphi_k\}$ = wavelet coefficients at scale δ
$\psi(x)$ = continuous wave envelope = $\Sigma_k \varphi_k \cdot \psi_\delta(x - k\delta)$
where ψ_δ is the "mother wavelet" (FPW Brillouin zone characteristic function)
Consequence: wavelet-based numerical PDE solvers (adaptive mesh refinement,
multigrid) are implicitly FPW calculations — they compute at scale δ and
extrapolate toward the IPW limit $\delta \to 0$.

4. Finitesimally Punctured Surfaces (FPS) and Manifolds (FPM)

Moving from the 1D FPW to 2D Finitesimally Punctured Surfaces (FPS) and n-dimensional Finitesimally Punctured Manifolds (FPM) opens an entirely new landscape of connections and applications.

4.1 Formal Definitions

Definition: Finitesimally Punctured Surface (FPS)

A smooth 2-manifold M with a finite or countable set $P = \{p_1, p_2, ...\}$ of puncture points, each replaced by a finite-size disk of radius $\delta > 0$.

The FPS is $M_\delta = M \setminus \{\text{disks of radius } \delta \text{ around each } p_n\}$.

Neutrosophic decomposition:

T-region: smooth M away from punctures (classical differential geometry)

F-region: puncture disks of radius δ (concentrated curvature)

I-region: annular transition zones of width ~ δ around each puncture

Definition: Finitesimally Punctured Manifold (FPM)

An n-dimensional smooth Riemannian manifold $M_\delta = (M \setminus P_\delta, g_\delta)$

where P_δ is a set of n-balls of radius δ removed from M,

and g_δ is the Riemannian metric on $M \setminus P_\delta$ together with distributional

curvature extensions at the boundary of each removed ball.

FPW (n=1) → FPS (n=2) → FPM (n≥3): unified hierarchy of punctured structures.

4.2 FPS Curvature: Smooth-to-Puncture Transition

On a FPS, the Gaussian curvature K transitions from the smooth background value K_0 to a sharply peaked value near each puncture. The FPS curvature distribution is:

Eq. (4.1) — FPS Curvature and Neutrosophic Euler Characteristic
$K_{FPS}(x) = K_{smooth}(x) + \Sigma_n \kappa_n \cdot f_\delta(x - p_n)$
where f_δ is a smooth bump function of width δ:
$f_\delta(x - p_n) \to \delta(x - p_n)$ as $\delta \to 0$ (recovers the IPM delta-function)
f_δ is smooth and bounded for $\delta > 0$ (FPS is everywhere smooth)
Neutrosophic Euler Characteristic:
$\chi_N(FPS) = (T, I, F)$
$T = \iint_{M_T} K_{smooth}\, dA$ (classical smooth contribution)
$I = \iint_{M_I} K_\varepsilon\, dA$ (transition-zone contribution, ~ $N\cdot(\delta/R)^2$)
$F = \iint_{M_F} K_\delta\, dA$ (puncture-disk contribution)

For a sphere with n punctures of radius δ:

$$\chi_N = (2 - 2n(\delta/R)^2,\ n\cdot(\delta/R)^2\cdot\delta K,\ n\cdot(\delta/R)^2)$$

4.3 Graphene and 2D Materials as FPS

Graphene — a single atomic layer of carbon atoms in a hexagonal lattice with lattice constant a = 0.142 nm — is precisely a Finitesimally Punctured Surface with δ = a in a hexagonal arrangement. The key results:

Eq. (4.2) — Graphene as FPS: Tight-Binding to Dirac Equation

Graphene as FPS:

$\delta = a = 0.142$ nm (C-C bond length)

FPS lattice: hexagonal with two atoms per unit cell

Dirac equation for electrons in graphene:

$$H \cdot \Psi = v_F \cdot (\sigma_x \cdot p_x + \sigma_y \cdot p_y) \cdot \Psi$$

where $v_F \approx c/300$ (Fermi velocity)

This emerges as the continuum limit ($\delta \to 0$) of the FPS tight-binding Hamiltonian:

$$H_{FPS} = -t \cdot \Sigma_{\langle i,j\rangle} (c_i^\dagger c_j + h.c.)$$

where $t \approx 2.8$ eV is the nearest-neighbor hopping integral

Topological defects in graphene = FPS punctures with non-zero κ_n curvature.

Each defect creates a bound state (discrete eigenvalue of FPS Dirac operator) — observed.

Graphene FPS — Hexagonal Lattice

A B A B

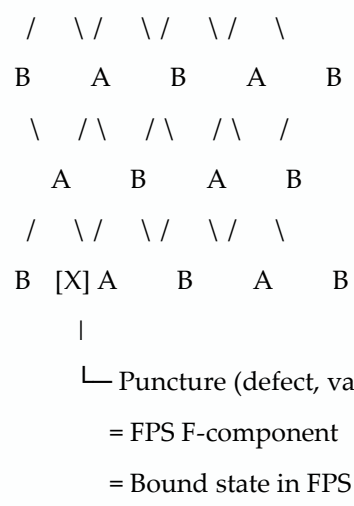

δ = a = 0.142 nm (C-C bond = FPS lattice spacing)

q_max = π/δ ≈ 22 nm^{-1} (Brillouin zone boundary = FPS UV cut-off)

Figure 2. Graphene as a Finitesimally Punctured Surface. The hexagonal lattice with spacing δ = 0.142 nm realizes an FPS. Vacancies and Stone-Wales defects are FPS punctures (F-component) that generate localized bound states.

4.4 String Worldsheets as FPS

In string theory, a fundamental string sweeping through spacetime traces a 2D worldsheet described by a conformal field theory (CFT). If the worldsheet is a FPS with puncture spacing δ_ws, the CFT acquires a natural UV cut-off at k_max = π/δ_ws, potentially replacing the need for the string length l_s as an independent UV regulator:

Eq. (4.3) — String Worldsheet as FPS
String worldsheet as FPS:
Polyakov action: $S = -(T_s/2) \int d^2\sigma \sqrt{h} \cdot h^{ab} \cdot \partial_a X^\mu \cdot \partial_b X_\mu$
FPS modification: replace $\int d^2\sigma$ by discrete sum over FPS lattice sites
FPS UV cut-off: $k_{max} = \pi/\delta_{ws}$ replaces string length $l_s = 1/\sqrt{(2\pi T_s)}$
Correspondence: $\delta_{ws} \leftrightarrow l_s$ (FPS spacing = string length)
FPS punctures: string interactions (splitting/joining vertices)

4.5 Riemannian Manifolds: FPM Ricci Flow

The Ricci flow (Hamilton, Perelman) evolves a Riemannian metric according to $\partial g_{ij}/\partial t = -2R_{ij}$, smoothing curvature inhomogeneities over time. Perelman used it to prove the Poincaré conjecture. On a FPM, the Ricci flow must be modified to prevent puncture neighborhoods from collapsing to zero size:

Eq. (4.4) — FPM Puncture-Regulated Ricci Flow
FPM Puncture-Regulated Ricci Flow:
$\partial g_{ij}/\partial t = -2R_{ij} + \Sigma_n \kappa_n(t) \cdot f_\delta(x - p_n) \cdot g_{ij}$
where the second term (Puncture Buffering) prevents collapse of δ-neighborhoods.
Standard Ricci flow: recovered as $\delta \to 0$ (punctures shrink to IPM delta-functions)
New result (FPM): for $\delta > 0$, the flow cannot develop finite-time singularities
at puncture points — the δ-neighborhoods remain stable.
Application: smooth resolution of orbifold singularities in string
compactifications; FPM replaces orbifold fixed points.

4.6 Knot Theory and Topological Quantum Computing

In topological quantum computing (Kitaev, Freedman), qubits are encoded in the braiding statistics of anyons — quasi-particles in 2D materials whose non-Abelian exchange generates topological quantum gates. In FPS language:

- Anyons = FPS punctures (finite-size quasi-particle defects with radius δ ~ lattice constant)
- Anyon braiding = holonomy of parallel transport around FPS punctures
- Non-Abelian statistics = non-Abelian holonomy group of the FPS connection
- Fault tolerance = topological protection, unchanged by continuous deformations of the braid path

Topological Quantum Computing as FPS Holonomy

Initial state: ① ② (two anyon-punctures on FPS)

Braiding operation: ① Anyon ① travels around ②

↓ ↗↘ ↑ tracing a path on the FPS

②

Result: $|\psi\rangle \rightarrow U_{braid} \cdot |\psi\rangle$ where U_{braid} = FPS holonomy matrix

Classical FPS limit ($\delta \rightarrow 0$): point anyons, exact topological gate

FPW realization ($\delta > 0$): finite-size anyons, corrections ~ $(\delta/\lambda_{dB})^2$

Figure 3. Anyon braiding as FPS holonomy. The quantum gate implemented by braiding depends only on the topology of the path, not its geometry — making topological quantum computers intrinsically fault-tolerant.

5. New Applications of FPW / FPS / FPM

5.1 Metamaterials with Engineered Neutrosophic Properties

Metamaterials achieve electromagnetic properties not found in natural materials (negative refractive index, perfect lensing, cloaking) by engineering the unit cell size and geometry. The FPW framework suggests a new class of Neutrosophically engineered metamaterials where the T, I, F components of the wave response are independently controllable:

Component	Physical Role in Metamaterial	Engineering Parameter
T (Truth)	Wave transmission; real part of refractive index n'	Unit cell geometry, resonator shape
F (Falsity)	Wave absorption/reflection; imaginary part n''	Resistive loading, loss tangent
I (Indeterminacy)	Random scattering at δ-scale defects	Controlled disorder, defect density

By engineering all three components independently, one can design materials with unprecedented wave-control capabilities: for example, a material that transmits (T = 1) a specific frequency band, reflects (F = 1) another, and scatters indeterminately (I = 1) a third — all in the same physical structure.

5.2 FPW-Based Quantum Error Correction

Standard quantum error correction protects against bit-flip ($|0\rangle \rightarrow |1\rangle$) and phase-flip ($|+\rangle \rightarrow |-\rangle$) errors. The FPW Neutrosophic qubit introduces a third error type:

Eq. (5.1) — Neutrosophic FPW Qubit and Three Error Types
Standard qubit: $\quad |\psi\rangle = \alpha|0\rangle + \beta|1\rangle \quad$ with $|\alpha|^2 + |\beta|^2 = 1$
Neutrosophic FPW qubit: $|\psi\_N\rangle = T|0\rangle + I|?\rangle + F|1\rangle$
where $|?\rangle$ = indeterminate state (neither $|0\rangle$ nor $|1\rangle$)
Physical meaning: qubit fell into FPW I-zone (transition between lattice cells)
Occurs when: qubit energy splitting ≈ thermal energy (kT)
FPW Error Types:
Type 1 (bit-flip): $\quad |0\rangle \rightarrow |1\rangle \quad$ (T → F)
Type 2 (phase-flip): $\quad |+\rangle \rightarrow |-\rangle \quad$ (phase rotation)
Type 3 (indeterminacy): $\quad |0\rangle$ or $|1\rangle \rightarrow |?\rangle$ (T or F → I)
FPW error correction codes must include the $|?\rangle$ syndrome to detect Type 3 errors.

5.3 FPW Signal Processing: Beyond Nyquist

The Nyquist-Shannon sampling theorem requires sampling rate ≥ 2B for a signal of bandwidth B. The FPW provides both a physical implementation (lattice spacing δ gives natural sample rate 1/δ) and a beyond-Nyquist framework. Because the FPW sub-particle distribution is sparse (N sub-particles along a wave of length L >> Nδ), compressed sensing techniques apply:

Eq. (5.2) — FPW Signal Processing and Compressed Sensing
FPW Nyquist frequency: f_N = 1/(2δ) (Brillouin zone boundary)
FPW signal capacity: N = L/δ sub-particles per wave of length L
Compressed sensing recovery (for sparse FPW):
Given M measurements (M << N), recover full {φ_k} by solving:
min ‖φ‖_1 subject to y = A · φ and M ≥ C · s · log(N/s)
where s = number of non-zero sub-particles (sparsity)
A = measurement matrix (random projections of FPW)
Application: FPW-inspired compressed sensing algorithms that exploit
the physical sparsity of sub-particle distributions.

5.4 FPW Cosmology: Dark Matter as FPW Solitons

If dark matter consists of FPW solitons — stable, localized excitations of a dark-sector FPW field — the dark matter particle mass is determined by the FPW spacing:

Eq. (5.3) — Dark Matter as FPW Solitons
FPW soliton mass: m_DM = $\hbar$ / (δ_dark · c)
FPW soliton de Broglie wavelength: λ_dB = δ_dark
Fuzzy dark matter (ultralight axions):
m_DM ~ 10^{-22} eV → δ_dark ~ $\hbar$c/m_DM ~ 1 kpc (kiloparsec)
Standard WIMP dark matter:

m_DM ~ 100 GeV → δ_dark ~ $\hbar c/m_{DM} \sim 2 \times 10^{-18}$ m
FPW primordial power spectrum cut-off:
P(k) has hard cut-off at $k_{max} = \pi/\delta_{dark}$
This suppresses power at large angular scales (low CMB multipoles)
— potentially explaining the observed low-l CMB power deficit.

5.5 Neural Networks as FPW: Spectral Bias

A deep neural network is, mathematically, a discrete function approximator on a finite lattice of neurons — a FPW of information processing. The FPW framework gives the spectral bias of neural networks a geometric interpretation:

Eq. (5.4) — Neural Network as FPW: Spectral Bias from FPW Dispersion
Neural network as FPW:
Network depth ↔ FPW lattice extent (number of sub-particles)
Network width ↔ number of parallel FPW channels
Activation function ↔ FPW nonlinear self-interaction $g\|\varphi_k\|^2$
FPW dispersion → Neural network spectral bias:
$\omega_{NN}(q) = (2J/\hbar)[1 - \cos(q\delta_{layer})]/\delta_{layer}^2$
where δ_{layer} = effective spacing between network layers
The neural network cannot represent frequencies above:
$f_{max} = 1/(2\delta_{layer})$ (FPW Nyquist limit of the network architecture)
Training the network changes δ_{layer} — it is a physical FPW renormalization
group flow: coarser → finer lattice as training progresses.

5.6 FPM Lattice Cryptography

The most promising post-quantum cryptographic systems (CRYSTALS-Kyber, CRYSTALS-Dilithium, FALCON, NTRU) are based on the hardness of lattice problems — the Learning With Errors (LWE) problem and the Shortest Vector Problem (SVP) on integer lattices. These cryptographic lattices are FPMs: finite-dimensional integer lattices with spacing $\delta = 1$ (in normalized units). The FPM Neutrosophic Euler characteristic encodes the security parameters:

Eq. (5.5) — FPM Cryptographic Lattices: Neutrosophic Security Structure
Cryptographic FPM security structure:
$\chi_N(\text{crypto lattice}) = (T, I, F)$
T-component: lattice regularity (easy to solve → large T → insecure)
F-component: lattice irregularity (hard to solve → large F → secure)
I-component: LWE noise parameter e (indeterminate error added to lattice)
LWE problem: given $(A, b = As + e \bmod q)$, find s
FPM interpretation: find the FPM puncture distribution $\{p_n = s_n\}$
given noisy measurements b at each FPM site
Security reduction: difficulty of SVP ↔ F-component magnitude of χ_N
New geometric tool: FPM topology may yield new hardness proofs or new attacks.

5.7 Biological Physics: FPS Membranes

The plasma membrane of a biological cell is a 2D fluid of lipid molecules with characteristic spacing $\delta \sim 0.8$ nm (lipid headgroup spacing) — a Finitesimally Punctured Surface. Membrane proteins are FPS punctures, and membrane dynamics are FPS wave modes:

Eq. (5.6) — Cell Membrane as FPS: Helfrich Mode Dispersion

Cell membrane as FPS:
δ = lipid headgroup spacing ≈ 0.8 nm
Helfrich undulation mode dispersion (FPS modification):
$\omega(k) = \kappa_b \cdot k^2 \cdot [1 - (k\delta)^2/12] / \eta$ for $k\delta \ll 1$
$\omega_{max} = \kappa_b \cdot (\pi/\delta)^2 / \eta$ (FPS UV cut-off)
κ_b = bending rigidity ≈ 20 kT
η = membrane viscosity
Membrane protein = FPS puncture with curvature $\kappa_n > 0$:
Creates bound state (localized lipid depletion zone of radius ~ δ)
Generates Aharonov-Bohm-type geometric phase for membrane waves
traveling around the protein — testable by single-molecule fluorescence.

6. The Grand FPW/FPS/FPM Correspondence Table

Table 1 summarizes the principal connections between the FPW/FPS/FPM program and established theories and applications, giving the FPW spacing δ where known.

Domain	**FPW/FPS/FPM Realization**	**δ Value**	**Key New Prediction**
Crystal lattice (phonons)	FPW (1D phonons)	0.1 – 0.5 nm	Debye cut-off = FPW Brillouin zone; $\omega_{max} = v_s \cdot \pi/\delta$
Graphene / 2D materials	FPS (2D Dirac fermions)	0.14 nm	Defects = FPS punctures; bound states at defect sites
Lipid membrane	FPS (Helfrich modes)	0.8 nm	Undulation mode cut-off at $\omega_{max} = \kappa_b(\pi/\delta)^2/\eta$

Photonic crystal	FPW (photon modes)	100 – 500 nm	Photonic band gap = FPW Brillouin zone boundary
Josephson array	FPW (plasma waves)	1 – 10 μm	Plasma mode band structure; discrete Shapiro steps
Lattice QCD	FPM (4D spacetime)	~ 0.1 fm	Continuum limit = FPM $\delta \to 0$; fermion doubling = I-zone
Topological insulator	FPS (surface states)	Lattice constant	Chern number = F-component of χ_N(FPS)
Topological qubits	FPS (anyon braiding)	~ nm	Braiding gate = FPS holonomy matrix; fault tolerance
Fuzzy dark matter	FPW (cosmological)	~ 1 kpc	Soliton mass $m \sim \hbar/(\delta c)$; CMB power cut-off at k_max
Loop quantum gravity	FPM (Planck lattice)	$l\_P \approx 1.6\times10^{-35}$ m	$\delta^2 = A\_min$(LQG); GW dispersion $\Delta\omega/\omega \sim (k\delta)^2$
AdS/CFT holography	FPM (bulk AdS)	l_P or l_s	Holographic RG = FPM continuum limit $\delta \to 0$
String worldsheets	FPS (worldsheet CFT)	l_s (string length)	CFT UV cut-off = FPS Brillouin zone; vertices = punctures
Neural networks	FPW (signal processing)	Layer spacing	Spectral bias = FPW dispersion; training = RG flow
Lattice cryptography	FPM (integer lattice)	1 (normalized)	Security = F-component of χ_N; LWE noise = I-component
Metamaterials	FPW/FPS (engineered)	Unit cell: nm–μm	Independent T, I, F control of wave response
Protein / drug binding	FPM (configuration space)	0.38 nm (amino acid)	Folding path = FPM geodesic; binding = FPW detection event

7. The Grand Unified Picture

The deepest implication of the FPW/FPS/FPM program is this: the distinction between "discrete" and "continuous" in physics is not ontological but scale-dependent. Every apparently continuous wave or

field is a FPW/FPS/FPM at some fundamental scale δ. The IPW is the mathematical ideal ($\delta \to 0$, the virtual world). The FPW/FPS/FPM is the physical reality ($\delta > 0$, the real world).

THE PUNCTURED WAVE HIERARCHY

VIRTUAL WORLD (Infinitesimal)	REAL WORLD (Finitesimal)
$\varepsilon \to 0$ (hyperreal)	$\delta > 0$ (real number)
▼	▼
IPW	FPW (1D, all wave types)
IPSu	FPS (2D: graphene, membranes, strings)
IPSp	FPM (nD: QCD, gravity, cryptography)

Limit connection: $FPW \to IPW$ as $\delta \to 0$

$FPS \to IPSu$ as $\delta \to 0$

$FPM \to IPM$ as $\delta \to 0$

Neutrosophic decomposition at every level:

T = smooth / wave / classical regime

F = puncture / particle / singular regime

I = transition zone of thickness δ

The I-zone is the only component that differs between IPW and FPW:

IPW: I is infinitesimally thin (virtual, unmeasurable)

FPW: I has finite thickness δ (real, measurable)

Figure 4. The IPW → FPW hierarchy: from the virtual to the real world. The FPW/FPS/FPM framework covers all known discrete structures in physics.

This means the FPW/FPS/FPM program is not proposing one new theory but a new meta-framework — a language in which all discrete structures in physics (crystals, lattices, graphs, spin networks, causal sets, neural networks, cryptographic lattices) are recognized as instances of the same geometric object (the FPM), and in which their common properties (Brillouin zones, topological invariants,

dispersion relations, UV cut-offs) follow from the same mathematical source: the FPM geometry and its Neutrosophic T-I-F decomposition.

8. Open Questions and Future Research Directions

The FPW/FPS/FPM program, while rich in connections and applications, raises many open questions that constitute a research agenda for the coming years:

1. The value of δ for fundamental particles. What is the FPW spacing δ for electrons, photons, and quarks? The FPW program predicts a modified electron g-factor: $g_{IPW} = g_{QED} + (\alpha/\pi)(\delta/l_C)^2$, where $l_C = \hbar/(mc)$ is the Compton wavelength. Current experimental limits suggest $\delta < 10^{-18}$ m. Next-generation Penning trap experiments may push this bound toward the classical electron radius $r_e \approx 2.8$ fm.
2. Deriving the Born rule from FPW first principles. Standard QM takes $P(x) = |\psi(x)|^2$ as a postulate. The FPW gives it a natural statistical interpretation (probability ∝ sub-particle density), but a rigorous first-principles derivation — analogous to Everett's derivation in Many Worlds — remains open.
3. Extension to fermions and gauge fields. The DNLSE (Eq. 2.1) describes scalar (spin-0) fields. A FPW Dirac equation (for spin-1/2 fields) and a FPW Yang-Mills equation (for spin-1 gauge fields) need to be developed and studied for stability and phenomenological predictions.
4. FPS Ricci flow and topology change. Can the FPM puncture-regulated Ricci flow (Eq. 4.4) prove topological results beyond the Poincaré conjecture? In particular, can it handle manifolds with prescribed FPS singularity structures arising in string compactification?
5. Neutrosophic engineering of metamaterials. Can the three FPW components T, I, F be independently tuned in a physical metamaterial? What are the electromagnetic properties of a material with I > T and I > F — a predominantly indeterminate metamaterial?
6. FPW vacuum energy and the cosmological constant. The FPW vacuum is a sea of Planck-scale FPW fluctuations. The vacuum energy density is $\varrho_{vac} \sim \hbar c/\delta^4$. For $\delta = l_P$ this gives $\varrho_{vac} \sim \varrho_{Planck}$ — the QFT prediction. For δ slightly larger than l_P (as the FPW allows), ϱ_{vac} is suppressed, potentially addressing the cosmological constant problem.
7. FPW information theory and holography. The FPW sub-particle lattice has information capacity $N = L/\delta$ bits per unit length. This gives a 3D holographic bound (information ∝ Volume/δ^3) rather than the standard 2D Bekenstein-Hawking bound (∝ Area). Are these two bounds related? Can the FPW derive the Bekenstein-Hawking entropy from first principles?

8. FPS and FPM in machine learning. Can FPW-inspired neural network architectures — with explicit Brillouin zone boundaries and Neutrosophic T-I-F error types — outperform standard architectures on tasks requiring multi-scale or uncertainty-aware processing?

9. Conclusion

The Finitesimally Punctured Wave (FPW) — and its higher-dimensional generalizations FPS and FPM — constitutes a new meta-framework for discrete structures in physics and mathematics. Its central insight is simple and powerful: every apparently continuous wave or field conceals a discrete sub-structure at some scale $\delta > 0$, and this sub-structure is governed by the universal FPW dispersion relation and Neutrosophic T-I-F decomposition.

We have shown that the FPW/FPS/FPM program connects to an exceptionally broad range of established theories: condensed matter (crystal lattices, topological insulators, graphene), quantum field theory (lattice QCD, fermion doubling), quantum foundations (causal set theory, loop quantum gravity, non-commutative geometry, AdS/CFT), topology (Ricci flow, Chern-Weil theory, knot theory), signal processing (wavelet theory, compressed sensing), and computation (topological quantum computing, lattice cryptography, neural networks).

The program also opens entirely new application domains: Neutrosophically engineered metamaterials with independently controllable T-I-F wave response; FPW quantum error correction codes that handle indeterminacy errors in addition to bit- and phase-flip errors; FPW-inspired compressed sensing algorithms; FPW soliton dark matter models; and FPS descriptions of biological membranes and protein folding pathways.

The deepest philosophical point is that the FPW is not a new physical theory competing with quantum mechanics — it is a new ontological language for quantum mechanics. Every discrete structure in physics is already a FPW/FPS/FPM. The FPW framework simply makes this structure explicit, names it, equips it with a precise mathematical description and a Neutrosophic logical decomposition, and — by doing so — unifies a vast landscape of apparently disparate phenomena under a single conceptual roof.

From the virtual world to the real world — from ε to δ — the journey of the Punctured Wave program is, ultimately, the journey from the ideal to the measurable.

References

[1] Smarandache, F. "The Infinitesimally Punctured Wave: A Corpuscular Visualisation of Wave-Particle Duality." Neutrosophic Sets and Systems, Vol. 97, 2026, pp. 704–708.

[2] Smarandache, F. "Comparisons of IPW with Copenhagen and De Broglie-Bohm Interpretations, Neutrosophic QM, and Non-Linear Electromagnetics." Neutrosophic Sets and Systems, Vol. 98, 2026, pp. 85–92.

[3] Smarandache, F. "Infinitesimally Punctured Wave and the Spectrum of Physical Waves." Progress in Physics, Vol. 22, 2026, pp. 18–24.

[4] Smarandache, F. "Infinitesimally Punctured Physics and Extended Nonstandard Analysis." Progress in Physics, Vol. 22, 2026, pp. 34–42.

[5] Smarandache, F. From Infinitesimally Punctured Wave (IPW) to Finitesimally Punctured Wave (FPW). NSIA Publishing House, 2026. ISBN 978-1-59973-880-2.

[6] Smarandache, F. Infinitesimally Punctured Geometry. NSIA Publishing House, 2026. ISBN 978-1-59973-863-5.

[7] Smarandache, F. Infinitesimally Punctured Physics. NSIA Publishing House, 2026. ISBN 978-1-59973-855-0.

[8] Connes, A. Noncommutative Geometry. Academic Press, 1994.

[9] Maldacena, J. "The Large N Limit of Superstring Field Theories." International Journal of Theoretical Physics, 38, 1999, pp. 1113–1133.

[10] Bombelli, L., Lee, J., Meyer, D., Sorkin, R.D. "Space-Time as a Causal Set." Physical Review Letters, 59(5), 1987, pp. 521–524.

[11] Rovelli, C. Quantum Gravity. Cambridge University Press, 2004.

[12] Kitaev, A. "Fault-Tolerant Quantum Computation by Anyons." Annals of Physics, 303, 2003, pp. 2–30.

[13] Hamilton, R.S. "Three-Manifolds with Positive Ricci Curvature." Journal of Differential Geometry, 17, 1982, pp. 255–306.

[14] Perelman, G. "The Entropy Formula for the Ricci Flow." arXiv:math/0211159, 2002.

[15] Nielsen, H.B., Ninomiya, M. "Absence of Neutrinos on a Lattice." Nuclear Physics B, 185, 1981, pp. 20–40.

[16] Castro Neto, A.H. et al. "The Electronic Properties of Graphene." Reviews of Modern Physics, 81, 2009, pp. 109–162.

[17] Helfrich, W. "Elastic Properties of Lipid Bilayers." Zeitschrift für Naturforschung, 28c, 1973, pp. 693–703.

[18] Candès, E.J., Tao, T. "Near-Optimal Signal Recovery from Random Projections." IEEE Trans. Inf. Theory, 52(12), 2006, pp. 5406–5425.

[19] Lyubashevsky, V. et al. CRYSTALS-Dilithium Algorithm Specifications. NIST PQC Submission, 2022.

[20] Robinson, A. Non-Standard Analysis. North-Holland, Amsterdam, 1966.

[21] Zadeh, L.A. "Fuzzy Sets." Information and Control, 8, 1965, pp. 338–353.

[22] Smarandache, F. Neutrosophy: Neutrosophic Probability, Set, and Logic. American Research Press, 1998.

All IPW/FPW resources freely available at: https://fs.unm.edu/IPW/